American Mineralogist, Volume 88, pages 240–244, 2003

The crystal structure of synthetic autunite, $Ca[(UO_2)(PO_4)]_2(H_2O)_{11}$

ANDREW J. LOCOCK* AND PETER C. BURNS

Department of Civil Engineering and Geological Sciences, University of Notre Dame, 156 Fitzpatrick Hall, Notre Dame, Indiana 46556-0767, U.S.A.

ABSTRACT

Autunite, $Ca[(UO_2)(PO_4)]_2(H_2O)_{11}$, is amongst the most abundant and widely distributed of the uranyl phosphate minerals, yet because of its pseudo-tetragonal symmetry and rapid dehydration in air, the details of its symmetry, stoichiometry, and structure were previously uncertain. The crystal structure of synthetic autunite was solved by direct methods and refined by full-matrix least-squares techniques to agreement indices $R_1 = 0.041$, calculated for the 1497 unique observed reflections ($|F_o| \geq 4\sigma_F$), and $wR_2 = 0.119$ for all data. Autunite is orthorhombic, space group *Pnma*, $Z = 4$, $a = 14.0135(6)$, $b = 20.7121(8)$, $c = 6.9959(3)$ Å, $V = 2030.55(15)$ Å^3. The structure contains the well-known autunite type sheet with composition $[(UO_2)(PO_4)]^-$, resulting from the sharing of equatorial vertices of the uranyl square bipyramids with the phosphate tetrahedra. The calcium atom in the interlayer is coordinated by seven H_2O groups and two longer distances to uranyl apical O atoms. Two symmetrically independent H_2O groups are held in the structure only by hydrogen bonding. Bond-length-constrained refinement provided a crystal-chemically reasonable description of the hydrogen bonding.

INTRODUCTION

Autunite, $Ca[(UO_2)(PO_4)]_2(H_2O)_{11}$, has been recognized for at least 150 years (Brooke and Miller 1852). Owing to its pseudo-tetragonal symmetry and rapid dehydration in air (Sowder et al. 2000), the structure of autunite has never before been determined, and the nature of the interlayer configuration, H_2O content, and hydrogen bonding were unknown. Autunite is the namesake of the autunite and meta-autunite groups, which consist of ~40 hydrated uranyl phosphate and arsenate minerals (Finch and Murakami 1999). We are interested in the structures, chemistries, and stabilities of autunite-group minerals because of their significance to the environment. They form in abundance and impact the mobility of uranium in phosphate-bearing systems (Sowder et al. 1996), such as the Koongarra uranium deposit in Australia (Murakami et al. 1997). Autunite largely controls the mobility of uranium in soils contaminated by actinides, such as at the Fernald site in Ohio (Buck et al. 1996), and the K1300 locality of the DOE-K 25 site at Oak Ridge, Tennessee (Roh et al. 2000). Autunite-group minerals are bioprecipitated by *Citrobacter* sp., which is proposed for remediation of groundwater contaminated by heavy metals (Basnakova et al. 1998; Macaskie et al. 2000). They have been found in experiments involving bacteria extracted from the Waste Isolation Pilot Plant repository (Francis et al. 2000). Autunite-group minerals precipitate at reactive barriers that use phosphate to limit the transport of uranium in groundwater (Fuller et al. 2002), and their stabilities under vadose- and saturated-zone conditions may determine the long-term effectiveness of these remediation strategies.

Museum specimens designated as autunite are almost invariably meta-autunite; our experiments have shown that autunite is unstable in air, and will dehydrate within minutes, resulting in strained crystals that give very poor quality single-crystal diffraction data. We have developed a technique for the synthesis of superb crystals of autunite, and have collected X-ray diffraction data for a single crystal contained within its mother solution. This has permitted the full determination and refinement of its structure, and elucidation of a probable scheme of hydrogen bonding.

PREVIOUS STUDIES

On the basis of its crystal morphology and biaxial optical character, autunite was thought to have either orthorhombic or monoclinic symmetry by early workers (Goldschmidt 1918; Larsen and Berman 1934; Frondel 1958, and references therein). An X-ray diffraction study conducted by Beintema (1938) indicated that the structure of autunite is tetragonal, space group *I*4/*mmm*, $a = 6.989$, $c = 20.63$ Å (corrected from kX units to $a = 7.003$, $c = 20.67$ Å in Frondel 1958; see also Bunn 1961), with the measured a and b dimensions differing by less that 1%. Most modern compilations state autunite is tetragonal (e.g., Strunz and Nickel 2001; Gaines et al. 1997), which implies that its biaxial optical character is anomalous.

EXPERIMENTAL METHODS

Single crystals of autunite were grown over the course of four months by slow diffusion of 0.1 *M* $H_3PO_{4(aq)}$ and 0.1 *M* $UO_2(NO_3)(H_2O)_{6(aq)}$ into a Ca-bearing silica gel formed by the hydrolysis of a mixture (1:10) of $(CH_3O)_4Si_{(liq)}$ and 0.1 *M* $Ca(NO_3)_2(H_2O)_{4(aq)}$. The crystals are biaxial negative; $2V$ is ~30°. A suitable crystal was sealed in a glass capillary (0.5 mm external diameter) with a volume of its diluted growth solution, and mounted on a Bruker PLATFORM three-circle X-ray

* E-mail: alocock@nd.edu

TABLE 1. Atomic positions ($\times 10^4$), displacement parameters ($Å^2 \times 10^3$), unit-cell parameters, crystallographic parameters, and data statistics for synthetic autunite

	x	*y*	*z*	U_{eq}	Occupancy%	Wyckoff Position
U1	1250(1)	5412(1)	7498(1)	12(1)	100	8*d*
P1	1245(2)	5003(1)	2478(2)	13(1)	100	8*d*
Ca1	1251(2)	7500	4501(4)	29(1)	86.0(7)	4*c*
O1	1235(5)	4551(2)	7482(5)	26(1)	100	8*d*
O2	1250(4)	6278(2)	7472(5)	21(1)	100	8*d*
O3	1252(4)	5440(2)	733(7)	29(1)	100	8*d*
O4	373(4)	4560(4)	2451(5)	28(2)	100	8*d*
O5	2118(4)	4557(3)	2553(5)	32(2)	100	8*d*
O6	1206(4)	5452(2)	4226(7)	23(1)	100	8*d*
O7	7591(7)	2500	2851(13)	41(3)	100	4*c*
O8	2368(5)	6647(4)	3510(11)	72(2)	100	8*d*
O9	126(4)	6645(3)	3438(11)	63(2)	100	8*d*
O10	10002(9)	2500	2833(13)	55(3)	100	4*c*
O11	1263(6)	7500	757(11)	39(2)	100	4*c*
O12	3257(5)	6614(4)	–255(10)	62(2)	100	8*d*
O13	759(5)	3379(3)	243(10)	57(2)	100	8*d*
H1	7260(40)	2830(20)	2220(90)	50	100	8*d*
H2	1970(40)	6330(30)	4120(90)	50	100	8*d*
H3	2210(60)	6540(50)	2150(40)	50	100	8*d*
H4	330(50)	6191(14)	3350(100)	50	100	8*d*
H5	80(60)	6650(40)	2010(30)	50	100	8*d*
H6	10370(40)	2851(18)	2330(90)	50	100	8*d*
H7	1300(50)	7056(12)	440(100)	50	100	8*d*
H8	2720(40)	6740(40)	580(90)	50	100	8*d*
H9	3972(16)	6550(50)	–270(140)	50	100	8*d*
H10	680(50)	3819(16)	750(90)	50	100	8*d*
H11	1483(14)	3360(50)	220(130)	50	100	8*d*

Data Statistics

a (Å)	14.0135(6)	Crystal size	0.46 mm × 0.46 mm × 0.06 mm
b (Å)	20.7121(8)	R_{int}	0.098
c (Å)	6.9959(3)	Unique reflections	4318
V (Å^3)	2030.55(15)	Unique $\lvert F_o\rvert > 4\sigma_F$	1497
Space group	*Pnma*	Refinement method	Full-matrix least-squares on F^2
F(000)*	1760	Parameters varied	168
μ (mm^{-1})*	16.443	R_1 † for $\lvert F_o\rvert > 4\sigma_F$	0.041
D_{calc} (g/cm^3)*	3.167(1)	R_1 † all data	0.086
Radiation	Mo*K*α	wR_2 ‡ all data	0.119
Total reflections	29,471	Goodness of fit all data	0.944
Data range (θ)	2.91 to 34.50°	Max. min. peaks (*e*/Å^3)	3.66, –6.51
Unit-cell contents	4{Ca[$(UO_2)(PO_4)]_2(H_2O)_{11}$}		

Note: U_{eq} is defined as one third of the trace of the orthogonalized U_{ij} tensor.
* Calculated with full occupancy of all atomic positions.
† $R_1 = [\Sigma||F_o| - |F_c||]/\Sigma|F_o|$.
‡ $wR_2 = [\Sigma[w(F_o^2 - F_c^2)^2]/\Sigma[w(F_o^2)^2]]^{0.5}$, $w = 1/(\sigma^2(F_o^2) + (a \cdot P)^2$, $P = 1/3\ \max(0,F_o^2) + 2/3F_c^2$, $a = 0.0537$.

diffractometer operated at 50 keV and 40 mA and equipped with a 4K APEX CCD detector with a crystal to detector distance of 4.7 cm. A sphere of three-dimensional data was collected using graphite-monochromatized Mo*K*α X-radiation and frame widths of 0.3° inω, with count-times per frame of 5 seconds. Data were collected over the range $6° \le 2\theta \le 70°$ in 4.5 hours; comparison of the intensities of equivalent reflections measured at different times during data collection showed no significant decay. Determination of the unit cell (Table 1) was based upon the location of centered diffraction maxima from several hundred frames of data, and the final cell was refined using 6903 reflections and least-squares techniques. The *a* unit-cell dimension reported here is double that of earlier work; this larger dimension was confirmed by 683 observed ($I > 3\sigma$) reflections in the sphere of data. The intensity data were reduced and corrected for Lorentz, polarization, and background effects using the Bruker program SAINT. A semi-empirical absorption correction was applied by modeling the crystal as a plate and rejecting data within 3 degrees of the primary X-ray beam. This procedure lowered R_{int} for 5750 intense reflections from 0.381 to 0.089.

Systematic absences of reflections were consistent with space group *Pnma*. Scattering curves for neutral atoms, together with anomalous dispersion corrections, were taken from *International Tables for X-ray Crystallography* (Ibers and Hamilton 1974). The Bruker SHELXTL Version 5 series of programs was used for the solution and refinement of the crystal structure. The structure was solved in space group *Pnma* using direct methods and was refined based on F^2 for all unique data. A structure model including anisotropic displacement parameters for all non-hydrogen atoms converged, and gave an agreement index (R_1) of 0.041, calculated for the 1497 observed unique reflections ($\lvert F_o\rvert \ge 4\sigma_F$). The final value of wR_2 was 0.119 for all data using the structure-factor weights assigned during least squares refinement. An empirical correction factor for extinction refined to 0.0019(1). The atomic positional parameters and displacement parameters are given in Table 1, and selected interatomic distances and angles are in Table 2. Anisotropic dis-

TABLE 2. Selected interatomic distances (Å) and angles (°) for autunite, $Ca[(UO_2)(PO_4)]_2(H_2O)_{11}$

U1-O1	1.784(5)		
U1-O2	1.794(5)	O1-U1-O2	178.9(2)
U1-O3*	2.264(5)	O1-U1-O3*	91.79(15)
U1-O4†	2.276(6)	O1-U1-O4†	90.8(3)
U1-O5‡	2.289(6)	O1-U1-O5‡	92.3(3)
U1-O6	2.291(5)	O1-U1-O6	91.70(15)
<U1-0>	2.12		
P1-O3	1.519(5)	O3-P1-O4	110.7(3)
P1-O4	1.529(6)	O3-P1-O5	112.4(3)
P1-O5	1.534(6)	O4-P1-O5	106.0(3)
P1-O6	1.537(5)	O3-P1-O6	106.3(3)
<P1-0>	1.53	O4-P1-O6	110.1(3)
		O5-P1-O6	111.4(3)
Ca1-O8§	2.461(7)		
Ca1-O8	2.461(7)	O8§-Ca1-O8	91.8(3)
Ca1-O(7)‖	2.463(9)	O8§-Ca1-O7‖	78.0(3)
Ca1-O(9)	2.485(7)	O8§-Ca1-O9	146.2(3)
Ca1-O(9)§	2.485(7)	O8§-Ca1-O9§	78.9(2)
Ca1-O(10)‖	2.562(12)	O8§-Ca1-O10‖	129.9(2)
Ca1-O(11)	2.619(9)	O8§-Ca1-O11	73.4(2)
Ca1-O(2)	3.275(5)	O8§-Ca1-O2	137.2(3)
Ca1-O(2)§	3.275(5)	O8§-Ca1-O2§	67.9(2)
<Ca1-0>	2.68		

O7-H1	0.94(2)	H1···O12	1.93(2)	O7-H1···O12	162
O8-H2	0.96(2)	H2···O6	2.11(2)	O8-H2···O6	154
O8-H3	1.00(2)	H3···O12	2.24(2)	O8-H3···O12	124
O9-H4	0.99(2)	H4···O6	2.05(2)	O9-H4···O6	150
O9-H5	1.00(2)	H5···O13	1.97(2)	O9-H5···O13	147
O10-H6	0.96(2)	H6···O13	1.91(2)	O10-H6···O13	151
O11-H7	0.95(2)	H7···O2	2.63(2)	O11-H7···O2	141
O12-H8	0.99(2)	H8···O11	2.57(2)	O12-H8···O11	143
		H8···O8	2.12(2)	O12-H8···O8	136
O12-H9	1.01(2)	H9···O9	2.07(2)	O12-H9···O9	139
O13-H10	0.98(2)	H10···O4	1.99(2)	O13-H10···O4	163
O13-H11	1.02(2)	H11···O8	2.00(2)	O13-H11···O8	144

Note: Symmetry transformations used to generate equivalent atoms:
* *x*, *y*, *z* + 1.
† −*x*, −*y* + 1, −*z* + 1.
‡ −*x* + 1/2, −*y* + 1, *z* + 1/2.
§ −*x* + 1, −*y* + 1, −*z* + 1.
‖ *x*, −*y* + 3/2, *z*.
O-H···O angles were obtained from SHELXL and rounded to the nearest degree.

placement parameters and structure factors are given in Tables 3 and 4 respectively.[1]

Possible hydrogen atom positions were located in difference-Fourier maps calculated following refinement of the model. As is typical for uranium minerals, it was very difficult to locate the hydrogen atoms on the basis of the X-ray data alone. Hydrogen atoms were inserted into the model at positions consistent with weak peaks in the difference-Fourier maps, as well as expected hydrogen atom positions derived from crystal-chemical arguments. Their positions were refined using the constraint that O-H bond-lengths be ~0.96 Å and have fixed isotropic displacement parameters. It was necessary to constrain the separations of the H4-H5, H3-H8, H6-H6, and H1-H1 atom pairs to reasonable values (~1.5 Å). The refinement provided a crystal-chemically reasonable hydrogen bonding network.

[1]For a copy of Tables 3 and 4, Document item AM-03-021, contact the Business Office of the Mineralogical Society of America (see inside front cover of recent issue) for price information. Deposit items may also be available on the American Mineralogist web site at http://www.minsocam.org.

STRUCTURE DESCRIPTION

Autunite contains the well-known autunite-type sheet formed by the sharing of vertices between uranyl square bipyramids and phosphate tetrahedra, with composition $[(UO_2)(PO_4)]^-$ (Fig. 1). The interlayer contains Ca atoms coordinated by seven H_2O groups with bond-lengths in the range 2.461 to 2.619 Å (Table 2). The Ca site is also located 3.275 Å from uranyl ion O atoms of the sheets on either side; if these correspond to weak bonds they serve to link the sheets directly through the Ca atom. The Ca position refined to 86% occupancy; charge balance is interpreted to be maintained by oxonium, in analogy with chernikovite (Atencio 1988; Morosin 1978). There are two additional H_2O groups that are located in the interlayer where they are held in position only by hydrogen bonding.

Bond valence analysis was performed using the parameters of Burns et al. (1997) for $^{[6]}U^{6+}$, Brown and Altermatt (1985) for P and Ca, and Ferraris and Ivaldi (1988) for hydrogen. The bond valence sums at the U, P, and Ca sites are 6.11, 5.06 and 1.71 valence units, respectively. These results are consistent with formal valences of U^{6+}, P^{5+}, and Ca^{2+}. Proposed hydrogen bonds for autunite are provided in Table 2, and their contributions to the bond-valence sums of the anions (calculated from the donor to acceptor distances) are shown in Table 5. In most cases the acceptor anion for each hydrogen bond is unambiguous, and the hydrogen bond distances range from 1.91 to 2.24 Å for nine of the hydrogen bonds. The bond associated with H7 may be accepted by O2, but the long H-acceptor distance of 2.63 Å indicates that this interaction is very weak. There are two possible acceptor anions for the bond associated with H8, O8 at 2.12 Å and O11 at 2.57 Å. Both belong to H_2O groups that are bonded to Ca; their bond-valence requirements are met

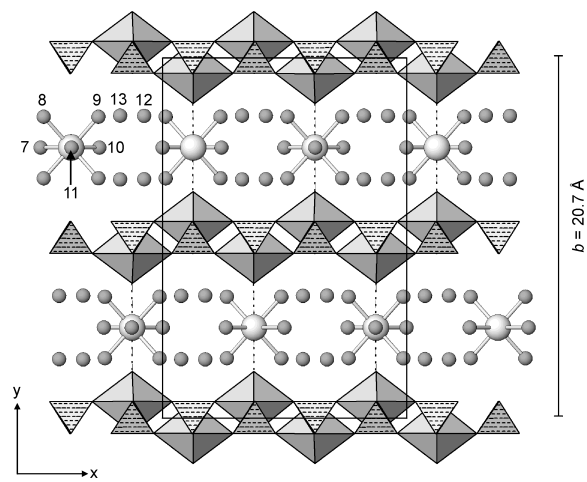

FIGURE 1. Polyhedral representation of the structure of autunite $Ca[(UO_2)(PO_4)]_2(H_2O)_{11}$, projected along [001]. The uranyl polyhedra are shown in gray and the phosphate tetrahedra are stippled. The Ca atoms are shown as large spheres, and the H_2O groups (with O atoms labeled) are shown as small spheres. The long interatomic distances from Ca to O_{Ur} (3.275 Å) are shown as dashed lines.

TABLE 5. Bond valence analysis for synthetic autunite (v.u.)

	O1	O2	O3	O4	O5	O6	O7	O8	O9	O10	O11	O12	O13	Total
U1	1.69	1.66	0.71	0.69	0.68	0.68								6.11
P1			1.30	1.27	1.25	1.24								5.06
Ca1		0.03 $^{x2\rightarrow}$					0.26	0.26 $^{x2\rightarrow}$	0.25 $^{x2\rightarrow}$	0.20	0.17			1.71
H1							0.83 $^{x2\downarrow}$					0.17		1.0
H2						0.13		0.87						1.0
H3								0.85				0.15		1.0
H4						0.14			0.86					1.0
H5									0.84				0.16	1.0
H6										0.81 $^{x2\downarrow}$			0.19	1.0
H7		0.08									0.92 $^{x2\downarrow}$			1.0
H8								0.15			0.08 $^{x2\downarrow}$	0.69		1.0
H9									0.15			0.85		1.0
H10				0.14									0.86	1.0
H11								0.15					0.85	1.0
Total	1.69	1.77	2.01	2.10	1.93	2.19	1.92	2.28	2.10	1.82	2.17	1.86	2.06	

essentially without the bond from H8. It is possible that the H8 bond is three-centered (bifurcated), with both the O8 and O11 atoms accepting the bond locally. Both O8 and O11 lie essentially in the same plane as O12 and H8; the sum of the O-H angles around H8 is 359°, consistent with a three-centered hydrogen bond arrangement (Jeffrey 1997).

The hydrogen bond network in autunite is illustrated in Figure 2. Hydrogen bonds extend from the H_2O groups to acceptors within the sheets, as well as to other H_2O groups located in the interlayer. The O2 uranyl ion O atom accepts the very weak H7 hydrogen bond. Three stronger hydrogen bonds extend from the H_2O groups to anions (O4 and O6) that are at the equatorial vertices of the uranyl square bipyramids, and that are also shared with the phosphate tetrahedra. Site O9 corresponds to a H_2O group bonded to a Ca atom, and accepts a single hydrogen bond. Sites O8 and O11 participate in a three-centered hydrogen bond from H8, and O8 accepts an additional hydrogen bond from H11. O12 and O13 each donate two hydrogen bonds and accept two hydrogen bonds, resulting in approximately tetrahedral coordination environments.

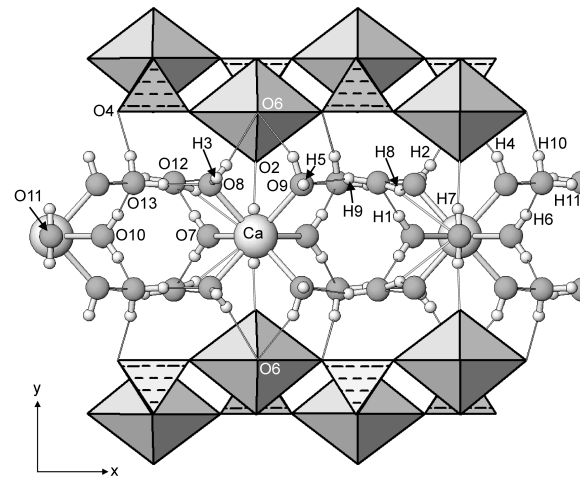

FIGURE 2. Projection of the structure of autunite $Ca[(UO_2)(PO_4)]_2(H_2O)_{11}$ along [001] showing the proposed hydrogen bonding network. The hydrogen atoms are shown as small pale gray spheres, the O atoms as large dark gray spheres, and the H···O bonds as thin rods; both possible H···O bonds for H8 are illustrated. The Ca-O_{Ur} interactions have been omitted for clarity. Only those O atoms participating in the hydrogen bonding network have been labeled. Note that a mirror plane parallel to the uranyl phosphate sheets passes through the plane of the Ca atoms.

DISCUSSION

Autunite dehydrates to meta-autunite rapidly in air (except at high relative humidity) (Sowder et al. 2000; Takano 1961). Loss of O12 and O13 from autunite results in the formula $Ca[(UO_2)(PO_4)]_2(H_2O)_7$. Details of the structure of meta-autunite are unclear, and there may be several different hydration states in nature. Collapse of the interlayer spacing is presumably associated with removal of H_2O groups from the interlayer, and strengthening of the interactions between the Ca cation and the uranyl ion O atoms within the sheets on either side. Our structure determination indicates that the Ca position in the interlayer is significantly underbonded, with only 1.71 valence units incident upon it, including the possible weak bonds to the uranyl ion O atoms. If these interactions are ignored, the bond-valence sum to Ca is only 1.65 valence units. We suggest that rapid dehydration of autunite in air is associated with the underbonding at the Ca site; removal of the O12 and O13 H_2O groups, coupled with collapse of the structure, will significantly increase the bond valence incident upon the Ca site because the interactions with the uranyl phosphate sheets should be enhanced.

ACKNOWLEDGMENTS

This research was supported by the Environmental Management Science Program of the Office of Science, U.S. Department of Energy, grant DE-FGO7-97ER14820. We thank S. Krivovichev, R. Finch, and an anonymous reviewer for their comments on the manuscript.

REFERENCES CITED

Atencio, D. (1988) Chernikovite, a new mineral name for $(H_3O)_2(UO_2)_2(PO_4)_2{\cdot}6H_2O$ superseding "hydrogen autunite." Mineralogical Record, 19, 249–252.

Basnakova, G., Stephens, E.R., Thaller, M.C., Rossolini, G.M., and Macaskie, L.E. (1998) The use of *Escheria coli* bearing a *phoN* gene for the removal of uranium and nickel from aqueous flows. Applied Microbiology and Biotechnology, 50, 266–272.

Beintema, J. (1938) On the composition and crystallography of autunite and the meta-autunites. Recueil des travaux chimiques des Pays-Bas, 57, 155–175.

Brooke, H.J. and Miller, W.H. (1852) Introduction to Mineralogy, p. 519. Phillips, London.

Brown, I.D. and Altermatt, D. (1985) Bond-valence parameters obtained from a systematic analysis of the inorganic crystal structure database. Acta Crystallographica, B41, 244–247.

Buck, E.C., Brown, N.R., and Dietz, N.L. (1996) Contaminant uranium phases and leaching at the Fernald Site in Ohio. Environmental Science and Technology, 30, 81–88.

Bunn, C.W. (1961) Chemical Crystallography, second edition. Oxford University Press, Oxford, Great Britain, pp. 130–131.

Burns, P.C., Ewing, R.C., and Hawthorne, F.C. (1997) The crystal chemistry of hexavalent uranium: polyhedron geometries, bond-valence parameters, and polymerization of polyhedra. Canadian Mineralogist, 35, 1551–1570.

Ferraris, G. and Ivaldi, G. (1988) Bond valence vs. bond length in O···O hydrogen bond. Acta Crystallographica, B44, 341–344.

Finch, R. and Murakami, T. (1999) Systematics and paragenesis of uranium minerals. Reviews in Mineralogy, 38, 91–180.

Francis, A.J., Dodge, C.J., Gillow, J.B., and Papenguth, H.W. (2000) Biotransformation of uranium compounds in high ionic strength brine by a halophilic bacterium under denitrifying conditions. Environmental Science and Technology, 34, 2311–2317.

Frondel, C. (1958) Systematic Mineralogy of Uranium and Thorium, U.S. Geological Survey Bulletin 1064, 400 p.

Fuller, C.C., Bargar, J.R., Davis, J.A., and Piana, M.J. (2002) Mechanisms of uranium interactions with hydroxyapatite: Implications for groundwater remediation. Environmental Science and Technology, 36, 158–165.

Gaines, R.V., Skinner, H.C.W., Foord, E.E., Mason, B., Rosenzweig, A., and King, V.T. (1997) Dana's New Mineralogy, Eighth Edition, 1819 p. Wiley, New York.

Goldschmidt, V. (1918) Atlas der Krystallformen, V, p. 5–6. Facsimile Reprint, 1986, Rochester Mineralogical Symposium, Rochester, New York.

Ibers, J.A. and Hamilton, W.C., Eds. (1974) International Tables for X-ray Crystallography, IV Revised and Supplementary Tables, vol. 4. The Kynoch Press, Birmingham, U.K.

Jeffrey, G.A. (1997) An Introduction to Hydrogen Bonding, p. 21–26. Oxford University Press, New York.

Larsen, E.S. and Berman, H. (1934) The Microscopic Determination of the Nonopaque Minerals, U.S. Geological Survey Bulletin 848, p. 162, 248.

Macaskie, L.E., Bonthrone, K.M., Yong, P., and Goddard, D.T. (2000) Enzymically mediated bioprecipitation of uranium by a *Citrobacter* sp.: a concerted role for exocellular lipopolysaccharide and associated phosphatase in biomineral formation. Microbiology, 146, 1855–1867.

Morosin, B. (1978) Hydrogen uranyl phosphate tetrahydrate, a hydrogen ion solid electrolyte. Acta Crystallographica, B34, 3732–3734.

Murakami, T., Ohnuki, T., Isobe, H., and Tsutomu, T. (1997) Mobility of uranium during weathering. American Mineralogist, 82, 888–899.

Roh, Y., Lee, S.R., Choi, S.K., Elless, M.P., and Lee, S.Y. (2000) Physicochemical and mineralogical characterization of uranium contaminated soils. Soil and Sediment Contamination, 9, 463–486.

Sowder, A.G., Clark, S.B., and Fjeld, R.A. (1996) The effect of silica and phosphate on the transformation of schoepite to becquerelite and other uranyl phases. Radiochimica Acta, 74, 45–49.

———(2000) Dehydration of synthetic autunite hydrates. Radiochimica Acta, 88, 533–538.

Strunz, H. and Nickel, E.H. (2001) Strunz Mineralogical Tables, Ninth Edition, 870 p. E. Schweizerbart'sche Verlagsbuchhandlung, Stuttgart, Germany.

Takano, Y. (1961) X-ray study of autunite. American Mineralogist, 46, 812–822.

MANUSCRIPT RECEIVED MARCH 10, 2002
MANUSCRIPT ACCEPTED OCTOBER 9, 2002
MANUSCRIPT HANDLED BY JEFFREY E. POST